GeoScience Engineering

TESTING POLYGON FOR SIMULATED VERTICAL DISPLACEMENT MEASUREMENTS BASED ON CO-LOCATED INSAR CORNER REFLECTOR AND GNSS STATION

Juraj STRUHÁR[1], *Michal KAČMAŘÍK*[1], *Ivana HLAVÁČOVÁ*[1], *Milan LAZECKÝ*[2,3], *Petr RAPANT*[1]
1 *VSB – Technical University of Ostrava, Faculty of Mining and Geology,*
Department of Geoinformatics, Ostrava, Czech Republic
2 *VSB – Technical University of Ostrava, IT4Innovations,*
Advanced Data Analysis and Simulations Lab, Ostrava, Czech Republic
3 *VSB – Technical University of Ostrava, Faculty of Civil Engineering,*
Department of Geotechnics and Underground Engineering, Ostrava, Czech Republic
E-mail: juraj.struhar@vsb.cz

ABSTRACT

With the growing availability of accurate and long-term measurements of displacements of technical infrastructure elements, there is a growing interest in the automated processing of acquired data. Various methods can be used for monitoring; however, radar interferometry and Global Navigation Satellite Systems (GNSS) measurements are among the best for long-term monitoring. GNSS allows for continuous monitoring of individual points, while radar interferometry allows only periodic data collection but with an areal coverage. Radar interferometry can also reach a better precision under certain conditions; therefore, it appears to be more appropriate. Automated systems are being developed that allow not only to process radar data but also to detect anomalies in vertical displacement. It is advisable to have a testing polygon for their verification, enabling the comparison of the automated processing of radar interferometry with an independent GNSS measurement. In autumn 2019, a testing polygon was built at the Department of Geoinformatics, HGF VSB – Technical University of Ostrava, consisting of three corner reflectors. Two are fixed, but one, complemented by a GNSS receiver, has an adjustable height. The article describes its construction and presents the first results of comparing automated radar interferometry processing with GNSS measurements.

Keywords: Corner reflector; Corner reflector and GNSS receiver co-location; Displacement monitoring; GNSS; InSAR; PS-InSAR; Sentinel-1; Testing polygon; Vertical displacement.

1 INTRODUCTION

With the growing availability of data for highly accurate measurements of the movement of ground structures, there is a growing interest in long-term automated monitoring of the movement of technical infrastructure features and issuing alerts in the event of a sudden change in the long-term trend of movement of a particular infrastructure object. In principle, such monitoring can be based either on standard geodetic methods like precise levelling [1], [2, 3], geotechnical monitoring [4, 5], GNSS measurements [6, 7, 8] or radar satellite data and their processing by one of the methods based on radar interferometry [9, 10, 11]. The advantage of using a GNSS method is a continuous absolute measurement of movements with relatively high accuracy; the disadvantages are the high purchase price, the need to equip each object of interest with a GNSS receiver, power line and an internet connection, and high operating costs of such a monitoring network, which essentially disqualifies the widespread use of GNSS monitoring. The advantage of radar interferometry is the high accuracy of measuring vertical movements (in the order of mm/year), areal coverage, no need to install special equipment on monitored objects (although possible), free availability of data and software, and lower operating costs. The disadvantages are a relative measurement in the satellite's slanted line of sight (LOS), only periodic data collection with a sampling

Vol. 67 (2021), No. 4
pp. 156–167, ISSN 1802-5420
DOI 10.35180/gse-2021-0061

rate of a few days, high demands on computing power, the requirement of expert knowledge and the need for direct visibility into the sky in a precise direction [12].

Therefore, a monitoring system based on radar interferometry is more suitable for practical use; GNSS can be used in the development phase to verify the correct functioning of the interferometric monitoring system.

Our research aimed to create a testing polygon that will permit controlled simulation of vertical movements of the building, monitoring them using radar interferometry and validating the accuracy of radar measurements by a second (independent) method, such as GNSS measurements.

2 TESTING POLYGON ESTABLISHMENT

Department of Geoinformatics at the VSB-Technical University of Ostrava (VSB-TUO) built a testing polygon in autumn 2019 in the area of the main university campus for practical testing of accuracy and reliability of interferometric measurements using Sentinel-1 radar data by comparing results with GNSS measurements. It consists of two stable and one adjustable corner reflector. Moreover, the adjustable corner reflector is complemented by a precise GNSS receiver. Given the size of the CR, there was concern about influencing GNSS measurements by multipath. Co-location of corner reflector and GNSS receiver was extensively studied by Community Safety and Earth Monitoring Division, Geoscience Australia [12], [13], [14]. Their experiments proved that the corner reflector has no significant effect on GNSS coordinates (less than 0.1 mm [14]) when a GNSS antenna is mounted above the corner reflector.

2.1 Selection of suitable locations for instruments installation

As the first step, it was necessary to identify suitable locations in the VSB-TUO university campus to install InSAR corner reflectors and the GNSS reference station. Following requirements were specified for a selection of suitable locations for a corner reflector (CR; adapted from [12]):

- the low intensity of backscatter of the locality to ensure at least 10dB difference between the backscatter intensity of a corner reflector and its background. According to Garthwaite et al. [15], the 10dB difference should allow reaching 1 mm precision of a single InSAR measurement while using the expected corner reflector design,
- good visibility from the satellite track,
- existence of a facility allowing a corner reflector installation while preventing it from damage or theft,
- reasonable mutual distance and orientation within all three corner reflectors,
- permission of university facility management to install a corner reflector at a locality.

For an adjustable construction complemented with a GNSS receiver, it was necessary to ensure also:

- good visibility over the sky,
- nearby indoor space with accessible electricity and network connection,
- possibility to install and secure the whole construction.

In order to evaluate backscatter intensity within the university campus, an intensity backscatter map was created individually for ascending and descending tracks of both A and B Sentinel-1 satellites. Maps were computed from Sentinel-1 images in VV polarization spanning 2015–2019 and represented mean backscatter intensity values. Backscatter intensity values were evaluated for thirteen locations (see Figure 1). Based on these results and the abovementioned requirements, three locations were finally selected for instrument installation, marked as CR1, CR2 and CR3+GNSS, see Figure 1.

Vol. 67 (2021), No. 4
pp. 156–167, ISSN 1802-5420
DOI 10.35180/gse-2021-0061

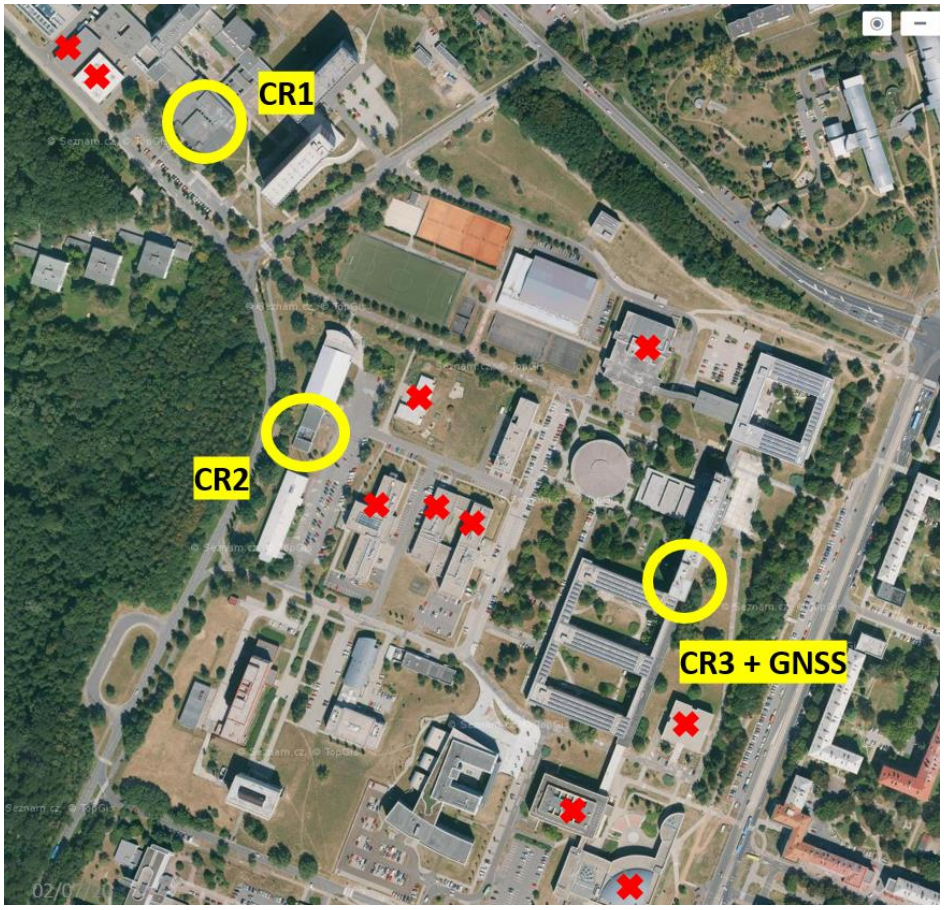

Figure 1. *Location of installed instruments in the VSB-TUO campus (yellow circles) and all other considered locations for corner reflector installation (red crosses)*

2.2 Design of instruments

Based on a realized analysis of backscatter intensity, previous experience with corner reflectors usage and available financial funds, the following design of a corner reflector was used:

- square trihedral shape, square base with a dimension of 75x75 cm,
- aluminium sheets with a thickness of 2.5 mm without any perforation,
- aluminium sheets are screwed on stable metal construction,
- fixed incident angle directed in between both descending tracks of Sentinel-1 satellites,
- possibility of turning in the horizontal direction,
- hole for water draining (to avoid its accumulation during rain).

The size and shape of the corner reflector significantly influence the strength of its backscatter intensity. While the uncomplicated square trihedral shape was chosen for construction reasons, the size of the square (75 cm) was selected mainly to get a difference between reflectance of the CR (Figure 2) and its background greater than 10 dB to achieve good accuracy in displacement trend estimation. Although there was an effort to use a bigger CR3 corner reflector, it was impossible since it could not be carried on the building roof through the interior. There was also a limitation in the load of the adjustable construction, allowing repetitive vertical movements holding the corner reflector and an antenna of the GNSS receiver. The production cost of a single used corner reflector was 400 EUR, including its bracket.

Vol. 67 (2021), No. 4
pp. 156–167, ISSN 1802-5420
DOI 10.35180/gse-2021-0061

Figure 2. *Used construction of corner reflector CR1*

As already mentioned, it was necessary to produce an adjustable device that would allow a repetitive vertical shift of construction holding a corner reflector and a GNSS antenna at the order of several millimetres. The adjustable construction was designed to meet the following requirements:

- allow repetitive vertical movement in up and down directions with a minimum step of 0.5 mm within at least 10 cm,
- ability to carry whole construction with CR and GNSS antenna,
- ability to resist strong wind, harsh weather conditions,
- not exceed the available budget.

The produced adjustable device shown in Figure 3 is based on four cylinders with inner tubes ensuring continuous vertical movement by mechanical handling. It was designed to carry the whole construction with a corner reflector of a square trihedral shape with a square base of up to 80x80 cm and a choke-ring GNSS antenna while resisting the effects of strong winds. The magnitude of forces acting on the adjustable device due to maximum expected wind speeds was calculated according to valid Czech regulations (technical standard ČSN EN 1991-1-4) and applied in the device design. The construction, including a solid base, adjustable device, corner reflector, and GNSS antenna, is placed on a building roof (see Figure 3).

Figure 3. *Detail of a produced adjustable device (left) and an overall look on a whole construction containing adjustable device, corner reflector and GNSS antenna (right)*

Vol. 67 (2021), No. 4
pp. 156–167, ISSN 1802-5420
DOI 10.35180/gse-2021-0061

2.3 Instruments installation

Three corner reflectors were installed on the university campus during autumn 2019. The CR3 was installed with a GNSS receiver (labelled as VSB1 hereafter). The second GNSS receiver was also available, located at the same building roof 50 m from VSB1. It is a permanent GNSS reference station labelled VSBO. Both VSB1 and VSBO were equipped with a geodetic grade GNSS receiver and a choke-ring antenna.

In general, corner reflectors, including large ones, can be installed on the ground, on a building wall or roof, on various existing objects (mast, pylon, bridge, railing, etc.). The particular way of installation always depends on specific options in the area of interest. To install the CR1 and CR2, a prepared iron bracket was attached to the sidewall of the selected building using a set of chemical anchors. The corner reflector was then fixed to this bracket with screws. This corner reflector installation can be used wherever a vertical wall is accessible, even for larger corner reflectors than the used ones. The adjustable device holding the CR3 and GNSS antenna was placed on a flat roof of the university building and screwed to a nearby guardrail to fix the whole construction and prevent its movement. Moreover, the base of the construction was heavily loaded with sandbags. Corner reflectors were oriented south-east to Sentinel-1 descending tracks (D51, D124) and were vertically pointed in between them. Approximate distances between locations with CRs were*:* CR1 to CR2: 340 m, CR2 to CR3: 270 m, CR1 to CR3: 550 m.

Figure 4 provides the time series of backscatter intensity values for locations of all three corner reflectors from August 2019 till July 2020. Plotted values represent a moving average of 5 consequent non-coregistered images, the date of corner reflector installation is marked with a red dashed line. An approximate increase of backscatter intensity for individual corner reflectors in the case of track 124 was: CR1 = +14dB, CR2 = +12dB, CR3 = +8dB. While CR1 and CR2 easily met the given requirement on a +10dB difference in backscatter intensity between the corner reflector and its background, the CR3 unfortunately did not due to a strong original backscatter of its surrounding. Because we did not have the possibility of another location of the CR3, amplitude correction was applied on the InSAR displacement measurements of the CR3 shown in this paper to eliminate the mixing corner reflector signal with its background.

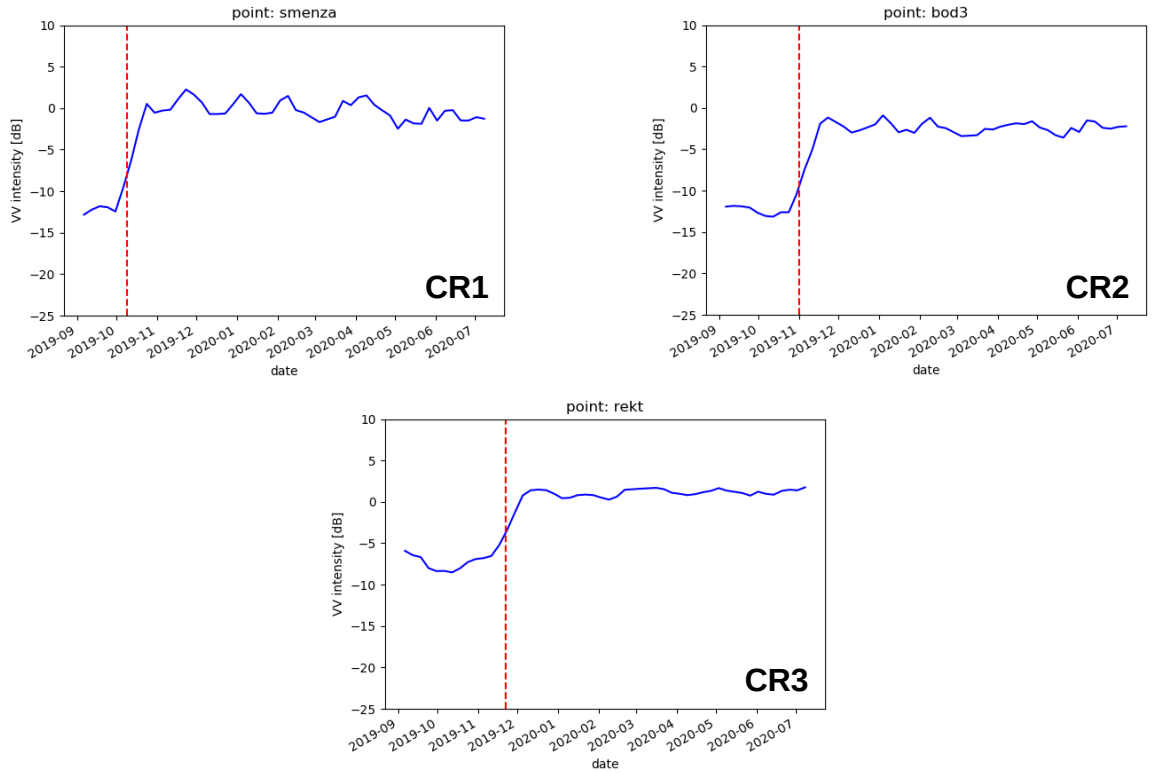

Figure 4. *Backscatter intensity time series for the location of CR1, CR2 and CR3. Values represent a moving average of 5 consequent non-coregistered images from track D124. Dashed red lines show a date of corner reflector installation*

Vol. 67 (2021), No. 4
pp. 156–167, ISSN 1802-5420
DOI 10.35180/gse-2021-0061

2.4 Design of experiment

The construction with CR3 and VSB1 GNSS antenna was regularly vertically shifted by 2.5 mm upwards once per month since the beginning of January 2020 to simulate a vertical movement of an infrastructure.

Sentinel-1 satellite data and GNSS observation data were continuously downloaded and processed for the year 2020 with the methods described in Section 4. Later, results achieved by both techniques were used to estimate the rate of annual vertical displacement.

3 INSAR AND GNSS DATA PROCESSING

Data processing was performed independently by two methods. Sentinel-1 data were processed by radar interferometry. A network solution based on double-differentiated observations was used for data of permanent GNSS stations.

3.1 InSAR

Satellite Synthetic Aperture Radar (SAR) interferometry (InSAR) is an established technology used to monitor deformations of large areas [16] or infrastructure [17]. Interferometry data processing requires the processing of at least two images. In the case of processing two images, it is possible to derive a digital surface model. Dynamic surface changes are monitored when processing multiple images, e.g. glacier movement, landslides, mining works, etc. To date, several radar interferometry-based methods have been developed, such as Differential SAR Interferometry (D-InSAR) and Multi-Temporal InSAR (MT-InSAR) methods, which can be classified into two categories: Small Baselines InSAR (SB-InSAR) and Persistent Scatter InSAR [18]. (PS-InSAR). We used the last mentioned method PS/InSAR [19], to test the built polygon.

The PSInSAR technique works with differential interferograms [19]. Its estimated accuracy is 1 mm/year [19], [20] for C-band SAR. This technique works most reliably on built-up surfaces, bare rocks and similar reflectors, and artificially created reflecting surfaces, e.g. corner reflectors. The result is a time series of measurements in line-of-sight (LOS). The results can be easily converted to vertical motion [21], while horizontal motion will be neglected. If multiple satellite orbits are used (minimum one descending and one ascending), the LOS motion can be decomposed into vertical and horizontal components [22].

Single Look Complex (SLC) radar Images from Sentinel 1A and 1B satellites were pre-processed in the ESA SNAP software, where the images were split into individual bursts covering the area of interest co-registered to the master image, and then interferograms were calculated. Other necessary input data such as perpendicular interferometric baselines, incidence angle, wavelength, SRTM DEM [23] and others were obtained from the interferogram metadata. Modified scripts from open-source SALSIT (Small Area Least-Squares InSAR Tool; https://insar.cz/salsit.html) were used to calculate PSInSAR. One of the modifications was the introduction of an estimate of the atmospheric phase and its subtraction from interferograms. In order to calculate PSInSAR, it was necessary to determine a stable reference point, and CR2 was chosen for this purpose.

InSAR processing was automated using our own set of developed scripts written in Python. It first downloaded the necessary radar images, covering the area of interest specified before processing as a polygon layer, using the OST (Open SAR Toolkit; https://github.com/ESA-PhiLab/OpenSarToolkit/blob/main/README.md). In the following steps, it started InSAR pre-processing, PSInSAR processing and post-processing one after the other. The output was an estimate of the velocity of movement and the time series of movement for each detected persistent scatters, in this case, corner reflectors.

Vol. 67 (2021), No. 4
pp. 156–167, ISSN 1802-5420
DOI 10.35180/gse-2021-0061

3.2 GNSS

GNSS data processing was realized in Bernese GNSS Software 5.2 [24] using the network solution based on double-differenced observations. A regional network of twenty GNSS reference stations located over Europe was set up (see Figure 5). Stations with longer distances to the Czech Republic were chosen to decorrelate station heights and tropospheric parameters that would be problematic while processing only short baselines. Parameters of GNSS processing are summarised in Table 1.

Table 1. *Basic parameters of GNSS processing*

Parameter	Value
GNSS systems used	GPS, GLONASS
precise products	CODE final [25]
elevation cut-off angle	3 degrees
elimination of the impact of the first-order ionospheric delay	ionosphere-free linear combination
interval of zenith total delay (ZTD)/horizontal tropospheric gradients parameters estimation	1 hour / 3 hours
tropospheric mapping function	VMF1 [26]
correction of antenna phase centre variations	absolute IGS14 model

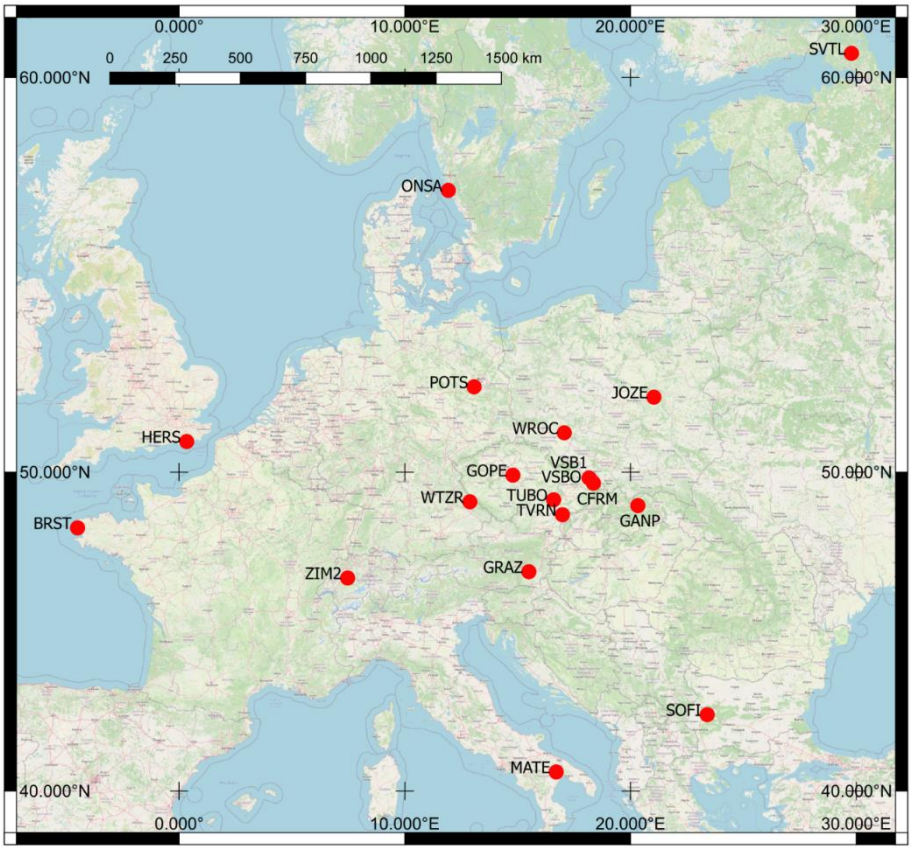

Figure 5*. A regional network of GNSS reference stations used for the processing*

Vol. 67 (2021), No. 4
pp. 156–167, ISSN 1802-5420
DOI 10.35180/gse-2021-0061

4 RESULTS

Changes in the height of adjustable construction with the CR3 and GNSS station VSB1 were estimated by the above described InSAR and GNSS data processing. The period between December 29, 2019, and December 29, 2020, was selected to estimate the annual linear rate of movement. The construction was moved upwards with a total shift of +30 mm (twelve times 2.5 mm) during this period. Period of an exact one year was selected to reduce the impact of building thermal dilation (expansion) on results since the CR3 was installed on a roof of 35 meters high building made of concrete and steel.

Figure 6 shows the time series of permanent GNSS station VSBO height and Figure 7 GNSS receiver VSB1 height. No smoothing or filtering of plotted daily height values was applied; occasional scattering is due to a lower quality of GNSS positioning on particular days or during short periods. While station VSBO showed very slow subsidence over the studied period (-1.9 mm/year), which can be rather attributed to an error of the measurements than to a real displacement, the height of VSB1 was steadily increasing as expected due to simulated movement.

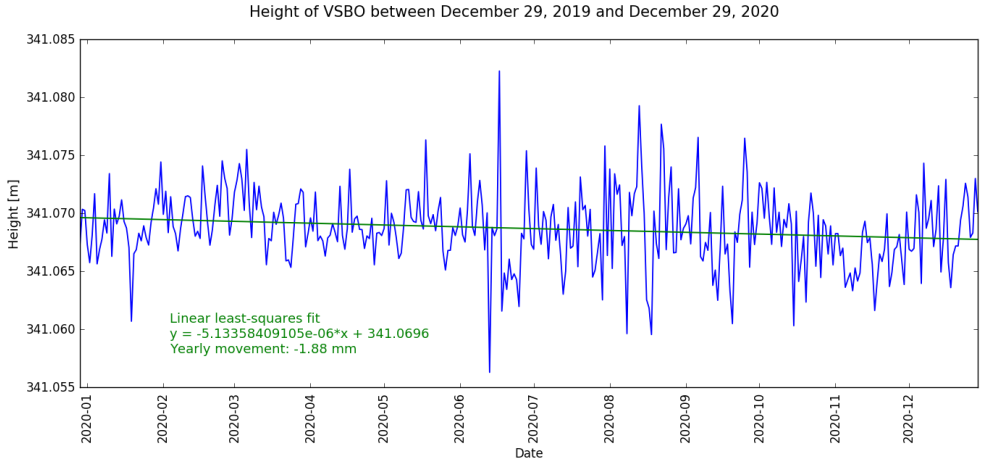

Figure 6. *Time series of the GNSS VSBO height between December 29, 2019, and December 29, 2020*

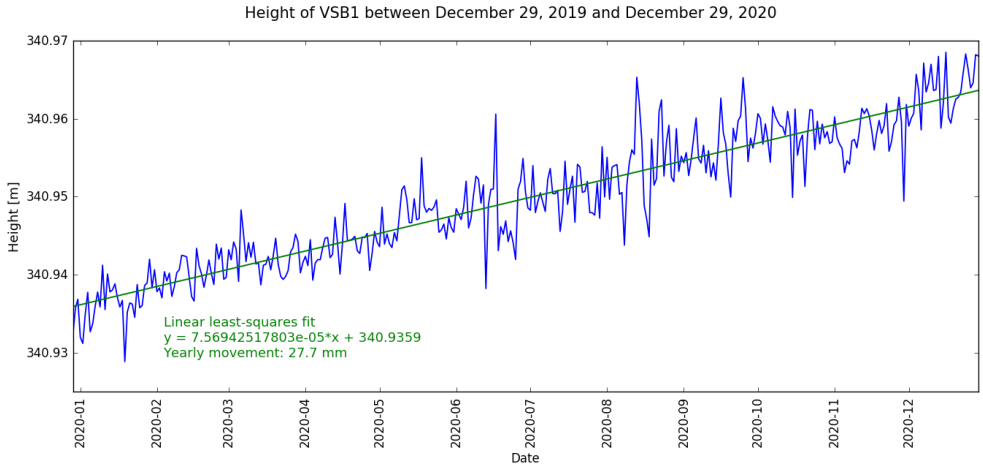

Figure 7. *Time series of the GNSS receiver VSB1 height between December 29, 2019, and December 29, 2020*

Vol. 67 (2021), No. 4
pp. 156–167, ISSN 1802-5420
DOI 10.35180/gse-2021-0061

Figure 8 shows a combination of VSB1 height and CR3 height estimated from two Sentinel-1 descending tracks by InSAR processing. Shown VSB1 heights represent a sliding median computed over 11 days. On top of them, realized changes in the construction height with CR3 and GNSS receiver VSB1 are plotted. It is important to note that these values, in contrast to results of InSAR and GNSS, were not affected by building thermal dilatation. Its influence can be visible from the InSAR time series with a slower increase of height during the first months of 2020 and reversely with a steeper increase during June and July 2020. As GNSS data from VSB1 and VSBO stations were processed using differential techniques, the impact of thermal dilatation on GNSS receiver VSB1 results were strongly suppressed. Thermal dilatation in InSAR displacement was also partially suppressed due to the Shenzen operation applied in the processing.

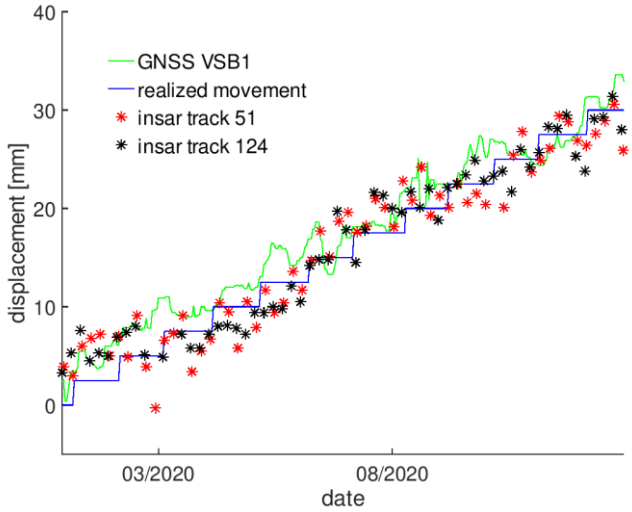

Figure 8. *Time series of CR3 height changes from two tracks of InSAR processing and GNSS receiver VSB1 height changes computed as sliding medians over 11 days. The period from December 29, 2019 till December 29, 2020*

To be able to quantify the results, the annual linear rate of movement was estimated using the least-squares method:

- InSAR, track D124: +27.6 mm per year,
- InSAR, track D51: +29.9 mm per year,
- GNSS: +27.7 mm per year (computed from all daily values shown in Figure 7).

As visible from the provided figures and estimates of the annual movement, outputs from both InSAR tracks agree very well with GNSS data processing and the actual total movement of +30 mm.

In the next step, a statistical comparison of height changes between both InSAR tracks, GNSS VSB1 and values of realized movement was performed, and its results are given in Table 2. To reduce the impact of lower precision of individual GNSS daily height estimates, sliding median computed over 11 days was used for GNSS VSB1. Correlation coefficients exceeded 0.9 in all comparisons; therefore, a strong positive correlation was found between all three sources – InSAR, GNSS, realized movement. Standard deviation (SDEV) comparisons between InSAR and GNSS were 2.8 mm in track D51 and 2.4 mm in track D124. About 0.3 mm lower SDEV values were obtained in comparisons between InSAR and the realized movement. Because outlying values strongly influence standard deviation as a measure of variability, lower values for InSAR comparisons would be achieved if occasionally occurring outliers were filtered out from the statistical evaluation. It was not applied in order to preserve all the InSAR data points. Visibly lower standard deviation values for comparison between GNSS and realized movement were reached only thanks to the applied median smoothing of original daily GNSS heights.

Vol. 67 (2021), No. 4
pp. 156–167, ISSN 1802-5420
DOI 10.35180/gse-2021-0061

Table 2. *Statistical comparison of InSAR and GNSS VSB1 results and the realized movement of CR3 from December 29, 2019 till December 29, 2020*

Track	Solutions compared	Standard deviation (mm)	Correlation coefficient	Number of images
D51	InSAR – realized movement	2.46	0.96	60
	InSAR – GNSS VSB1	2.81	0.94	
	GNSS VSB1 – realized movement	1.52	0.99	
D124	InSAR – realized movement	2.06	0.97	60
	InSAR – GNSS VSB1	2.37	0.96	
	GNSS VSB1 – realized movement	1.57	0.98	

5 CONCLUSIONS

A testing polygon was built in the area of the VSB-TUO university campus to make a simulation of vertical displacements and their estimation using two independent technologies: satellite radar interferometry utilizing Sentinel-1 imagery and GNSS measurements. The polygon mainly consists of an adjustable device that allows for vertical displacements simulation while holding a corner reflector and a GNSS antenna. Two fixed corner reflectors and one permanent GNSS reference station form the rest of the installed instruments. Both GNSS and InSAR data for the year 2020 were processed using state-of-the-art techniques to verify the quality of the established polygon and evaluate the performance of both technologies. A linear vertical displacement with a magnitude of 2.5 mm per month was simulated over the mentioned period. The results showed that both GNSS and InSAR can reach an accuracy of several millimetres in estimating the annual linear trend. Standard deviation computed from differences between InSAR individual height estimates and the GNSS height estimates oscillated around 2.5 mm depending on the used Sentinel-1 track. In the same comparison, the correlation coefficient reached 0.95.

Apart from estimating long-term displacement trend, GNSS and InSAR monitoring can be used to detect anomalous behaviour caused, i.e., a sudden height change. Due to the presence of noise in both GNSS and InSAR time series, estimation of anomalous behaviour should be instead based on a set of last measurements than on a single last value. A model established over a long-term time series can estimate the expected value (set of values) for the last measurement(s) and compare it with the obtained results to assess a potential anomaly. The built testing polygon can be used to simulate various anomalous behaviours in vertical displacement and to support the development of tools for their successful detection.

ACKNOWLEDGMENTS

This work was supported by Grant of SGS No. SP2020/48, Faculty of Mining and Geology, VSB – Technical University of Ostrava.

REFERENCES

[1] DERMANIS, A. Fundamentals of surface deformation and application to construction monitoring. *Applied Geomatics*. 2011, vol. 3(1), pp. 9–22. ISSN 1866-928X. DOI: 10.1007/s12518-010-0040-y

[2] GURA, D.A., N.M. KIRYUNIKOVA, E.D. LESOVAYA, N.I. KHUSHT, A.P. PAVLUKOVA and V.V. PODTELKOV. Geodetic Monitoring System to Ensure Safe Operation of Infrastructure Facilities. In: *2020 International Multi-Conference on Industrial Engineering and Modern Technologies (FarEastCon): October 6–9, 2020, Vladivostok, Russia*. 2020, pp. 1–6. DOI: 10.1109/FarEastCon50210.2020.9271604

[3] BRYN, M.J., D.A. AFONIN and N.N. BOGOMOLOVA. Geodetic Monitoring of Deformation of Building Surrounding an Underground Construction. *Procedia Engineering*. 2017, vol. 189, pp. 386–392. ISSN 1877-7058. DOI: 10.1016/j.proeng.2017.05.061

[4] OGUNDARE, J.O. Chapter 11 – Deformation Monitoring and Analysis: Geotechnical and Structural Techniques. *Precision Surveying: The Principles and Geomatics Practice*. John Wiley & Sons, 2016, pp. 377–440. ISBN 9781119102519. DOI: 10.1002/9781119147770.ch11

[5] SMITH, A. and N. DIXON. Listening for deterioration and failure: towards smart geotechnical infrastructure. *Proceedings of the Institution of Civil Engineers – Smart Infrastructure and Construction*. 2018, vol. 171(4), pp. 131–143. ISSN 2397-8759. DOI: 10.1680/jsmic.19.00019.

[6] BARZAGHI, R., N.E. CAZZANIGA, C.I. DE GAETANI, L. PINTO and V. TORNATORE. Estimating and Comparing Dam Deformation Using Classical and GNSS Techniques. *Sensors*. 2018, vol. 18(3), art. no. 756. ISSN 1424-8220. DOI: 10.3390/s18030756

[7] BELLONE, T., P. DABOVE, A.M. MANZINO and C. TAGLIORETTI. Real-time monitoring for fast deformations using GNSS low-cost receivers. *Geomatics, Natural Hazards and Risk*. 2016, vol. 7(2), pp. 458–470. ISSN 1947-5713. DOI: 10.1080/19475705.2014.966867

[8] XIAO, R., H. SHI, X. HE, Z. LI, D. JIA and Z. YANG. Deformation Monitoring of Reservoir Dams Using GNSS: An Application to South-to-North Water Diversion Project, China. *IEEE Access*. 2019, vol. 7, pp. 54981–54992. ISSN 2169-3536. DOI: 10.1109/ACCESS.2019.2912143

[9] BAKON, M., D. PERISSIN, M. LAZECKY and J. PAPCO. Infrastructure Non-linear Deformation Monitoring Via Satellite Radar Interferometry. *Procedia Technology*. 2014, vol. 16, pp. 294–300. ISSN 2212-0173. DOI: 10.1016/j.protcy.2014.10.095

[10] BIANCHINI CIAMPOLI, L., V. GAGLIARDI, C. FERRANTE, A. CALVI, F. D'AMICO and F. TOSTI. Displacement Monitoring in Airport Runways by Persistent Scatterers SAR Interferometry. *Remote Sensing*. 2020, vol. 12(21), art. no. 3564. ISSN 2072-4292. DOI: 10.3390/rs12213564

[11] ZHU, M., X. WAN, B. FEI, Z. QIAO, C. GE, F. MINATI, F. VECCHIOLI, J. LI and M. COSTANTINI. Detection of Building and Infrastructure Instabilities by Automatic Spatiotemporal Analysis of Satellite SAR Interferometry Measurements. *Remote Sensing*. 2018, vol. 10(11), art. no. 1816. ISSN 2072-4292. DOI: 10.3390/rs10111816

[12] PARKER, A.L., W.E. FEATHERSTONE, N.T. PENNA, M.S. FILMER and M.C. GARTHWAITE. Practical Considerations before Installing Ground-Based Geodetic Infrastructure for Integrated InSAR and cGNSS Monitoring of Vertical Land Motion. *Sensors*. 2017, vol. 17(8), art. no. 1753. ISSN 1424-8220. DOI: 10.3390/s17081753

[13] GARTHWAITE, M.C., M. HAZELWOOD, S. NANCARROW, A. HISLOP and J.H. DAWSON. A regional geodetic network to monitor ground surface response to resource extraction in the northern Surat Basin, Queensland. *Australian Journal of Earth Sciences*. 2015, vol. 62(4), pp. 469–477. ISSN 1440-0952. DOI: 10.1080/08120099.2015.1040073

[14] FUHRMANN, T., M.C. GARTHWAITE and S. MCCLUSKY. Investigating GNSS multipath effects induced by co-located Radar Corner Reflectors. *Journal of Applied Geodesy*. 2021, vol. 15(3), pp. 207–224. ISSN 1862-9024. DOI: 10.1515/jag-2020-0040

[15] GARTHWAITE, M.C., S. NANCARROW, A. HISLOP, M. THANKAPPAN, J.H. DAWSON and S. LAWRIE. The Design of Radar Corner Reflectors for the Australian Geophysical Observing System: A single design suitable for InSAR deformation monitoring and SAR calibration at multiple microwave frequency bands. Record 2015/03. *Geoscience Australia*. ISBN 978-1-925124-57-6. DOI: 10.11636/Record.2015.003

[16] WANG, G., Y. WANG, X. ZANG, J. ZHU and W. WU. Locating and monitoring of landslides based on small baseline subset interferometric synthetic aperture radar. *Journal of Applied Remote Sensing*. 2019, vol. 13(4), art. no. 044528. ISSN 1931-3195. DOI: 10.1117/1.JRS.13.044528

[17] MILILLO, P., D. PERISSIN, J.T. SALZER, P. LUNDGREN, G. LACAVA, G. MILILLO and C. SERIO. Monitoring dam structural health from space: Insights from novel InSAR techniques and multi-parametric modeling applied to the Pertusillo dam Basilicata, Italy. *International Journal of Applied Earth Observation and Geoinformation*. 2016, vol. 52, pp. 221–229. ISSN 0303-2434. DOI: 10.1016/j.jag.2016.06.013

[18] PEPE, A. and F. CALÒ. A Review of Interferometric Synthetic Aperture RADAR (InSAR) Multi-Track Approaches for the Retrieval of Earth's Surface Displacements. *Applied Sciences*. 2017, vol. 7(12), art. no. 1264. ISSN 2076-3417. DOI: 10.3390/app7121264

[19] FERRETTI, A.; C. PRATI and F, ROCCA. Permanent scatterers in SAR interferometry. *IEEE Transactions on Geoscience and Remote Sensing*. 2001, vol. 39(1), pp. 8–20. ISSN 1558-0644. DOI: 10.1109/36.898661

[20] FERRETTI, A., C. PRATI and F. ROCCA. Nonlinear subsidence rate estimation using permanent scatterers in differential SAR interferometry. *IEEE Transactions on Geoscience and Remote Sensing*. 2000, vol. 38(5), pp. 2202–2212. ISSN 1558-0644. DOI: 10.1109/36.868878

[21] LAZECKY, M., I. HLAVACOVA, M. BAKON, J.J. SOUSA, D. PERISSIN and G. PATRICIO. Bridge Displacements Monitoring Using Space-Borne X-Band SAR Interferometry. *IEEE Journal of Selected Topics in Applied Earth Observations and Remote Sensing*. 2016, vol. 10(1), pp. 205–210. ISSN 2151-1535. DOI: 10.1109/JSTARS.2016.2587778

[22] SAMIEIE-ESFAHANY, S., R.F. HANSSEN, K. VAN THIENEN-VISSER and A. MUNTENDAM-BOS. On the Effect of Horizontal Deformation on InSAR Subsidence Estimates. In: LACOSTE, H., ed. *Proceedings of Fringe 2009 Workshop: Advances in the Science and Applications of SAR Interferometry: November 30–December 4, 2009, Frascati, Italy*. ESA-SP vol. 677, 2010, pp. 1–7. Available from: https://articles.adsabs.harvard.edu/full/2010ESASP.677E..39S

[23] FARR, T.G., P.A. ROSEN, E. CARO, R. CRIPPEN, R. DUREN, S. HENSLEY, M. KOBRICK, M. PALLER, E. RODRIGUEZ, L. ROTH, D. SEAL, S. SHAFFER, J. SHIMADA, J. UMLAND, M. WERNER, M. OSKIN, D. BURBANK and D. ALSDORF. The Shuttle Radar Topography Mission. *Review of Geophysics*. 2007, vol. 45(2). ISSN 1944-9208. DOI: 10.1029/2005RG000183

[24] DACH, R., S. LUTZ, P. WALSER and P. FRIDEZ (eds.). *Bernese GNSS Software Version 5.2. User manual*. Bern: University of Bern, Astronomical Institute, 2015. ISBN 978-3-906813-05-9. DOI: 10.7892/boris.72297

[25] DACH, R., S. SCHAER, D. ARNOLD, M.S. KALARUS, L. PRANGE, P. STEBLER, A. VILLIGER and A. JÄGGI. *CODE final product series for the IGS [Dataset]*. Bern: University of Bern, Astronomical Institute, 2020. DOI: 10.7892/boris.75876.4

[26] BÖHM, J., B. WERL and H. SCHUH. Troposphere mapping functions for GPS and very long baseline interferometry from European Centre for Medium-Range Weather Forecasts operational analysis data. *Journal of Geophysical Research: Solid Earth*. 2006, vol. 111(B2), art. no. B02406. ISSN 2169-9356. DOI: 10.1029/2005JB003629